Driving sustainable energy storage: A multi-scale investigation of methane hydrate formation with green promoters and innovative reactor design

Ahmed Omran, Nikolay Nesterenko, Valentin Valtchev

Graphical Abstract

Driving Sustainable Energy Storage:A Multi-scale Investigation of Methane Hydrate Formation with Green Promoters and Innovative Reactor Design

Ahmed Omran, *Nikolay Nesterenko*, *Valentin Valtchev*

Highlights

Driving Sustainable Energy Storage:A Multi-scale Investigation of Methane Hydrate Formation with Green Promoters and Innovative Reactor Design

Ahmed Omran, *Nikolay Nesterenko*, *Valentin Valtchev*

- Green approach : H-SSZ-13, L-tryptophan, and reactor design boost hydrate kinetics.
- H-SSZ-13 zeolite excels with 10.5 min induction time, 115 V/V capacity at 283K.
- Fixed bed reactor with metallic filament packing revs up heat transfer and capacity.
- L-tryptophan outperforms at 283 K and 288 K in induction time and gas uptake.
- Hydrates showed minimal gas loss compared to LNG at for 4 months.

Driving Sustainable Energy Storage:A Multi-scale Investigation of Methane Hydrate Formation with Green Promoters and Innovative Reactor Design

Ahmed Omran[a,*], *Nikolay Nesterenko*[b], *Valentin Valtchev*[a,**]

[a]*Normandie Université, ENSICAEN, UNICAEN, Laboratoire Catalyse et Spectrochimie (LCS), 14050, Caen, France*

[b]*Gas Solutions GTB, Sulzer, 8401, Winterthur, Zurich, Switzerland*

Abstract

Synthetic Gas hydrates are promising materials for safe and compact energy storage but their wide-scale application is hindered by slow formation kinetics. We investigated the effect of green kinetic promoters of H-SSZ-13 zeolite, L-tryptophan, L-leucine, and L-methionine in a novel reactor design to accelerate hydrate formation at 6 MPa. In non-stirred reactor (NSR), H-SSZ-13 and L-tryptophan showed superior performance over L-leucine and L-methionine. While H-SSZ-13 showed the lowest average time taken for 90% completion of methane uptake (t_{90}) of 286 mins and the highest volumetric capacity of 115 V/V at 283 K, its kinetic performance, along with other promoters, dropped significantly at 293 K. We introduced a new fixed bed reactor (FBR) equipped with light metallic filament packing (MFP) to increase gas diffusion and thermal conductivity. The combined effect of FBR-MFP reactor with zeolite significantly improved the kinetics overcoming NSR drawbacks. At 293.15 K, H-SSZ-13 zeolite promoter showed superior performance reducing the induction time and t_{90} to 3 and 154 mins, respectively. Furthermore, it exploited 88.6%, and 96% of the sII clathrates volumetric storage capacity at 293 K and 283 K, respectively. Finally, we showed that the synthesized hydrates can be stored at atmospheric pressure for 4 months without significant methane loss. This multi-scale approach is paving the way for scaling up green and economical gas hydrate technology.

Keywords: Zeolitic ice, Acidic zeolite, Kinetic hydrate promoters, Promotion mechanism, Nucleation sites, Reactor Design, Amino acids, DFT

*Corresponding author

**Corresponding author

Email addresses: omran@ensicaen.fr (*Ahmed Omran*), valentin.valtchev@ensicaen.fr (*Valentin Valtchev*)

Nomenclature

Abbreviations

LNG	liquified natural gas
SGH	synthetic gas hydrate
KHP	kinetic hydrate promoter
SDS	sodium dodecyl sulfate
THF	tetrahydrofuran
FBR	fixed bed reactor
MFP	metallic filament packing
NSR	non-stirred reactor
DFT	density functional theory
ICP	inductively coupled-atomic plasma emission spectroscopy
EDX	energy dispersive X-ray
PXRD	powder X-ray diffraction
SEM	scanning electron microscopy

Notations/Symbols

H-USY	H-form ultrastable Y zeolite
H-SSZ-13	H-form SSZ-13 zeolite
ΔE^{HG}	host-guest interaction energy
t_{90}	time taken for 90% completion of methane uptake

Units

V/V	volume of gas (STP) /volume of hydrate
€/GWH/D	euros per gigawatt-hour per day

1. Introduction

The energy transition toward greener technologies is coupled with increasing global energy demand which poses the dilemma of balancing sustained economic growth and

maintaining the environmental goals toward reducing carbon emissions [1]. In that aspect, natural gas can play an important role as a "transitional fuel" on the way from traditional fossil fuels to green energy resources [2, 3]. Although it is considered a fossil fuel, it is much cleaner than traditional oil and coal resources. It thus has been recently labeled as a green and sustainable energy source by EU taxonomy regulations [4]. Concerning the hydrogen economy, one can find that methane is currently the main feedstock for hydrogen with steam methane reforming responsible for 48% of the global hydrogen demand compared to only 4% produced by electrolysis [5].

The natural gas supply chain has been extremely disturbed due to the recent pandemic and geopolitical developments. The current global energy crisis emphasized the need for economic methane transportation and long-term buffer storage that can absorb market shocks [6, 7]. Despite its high storage capacity, which can reach 600 volume of gas (STP) /volume of hydrate (V/V), the well-established gas transport technology of liquified natural gas (LNG) is limited by very high capital expenditure due to expensive infrastructure and energy-intensive cooling requirements suitable for short-term storage [8]. Moreover, LNG needs large reserves and long-term contracts to reduce operational costs, which has been proven insufficient to meet the current increasing demand or sudden market shocks [9, 10].

The "zeolitic ice" or synthetic gas hydrate (SGH) is considered a promising alternative that allows physical methane storage in water through a safe, stable, compact solid form with a possibility of almost full methane recovery ~~[11, 12]~~[1, 11, 12]. Due to its simple and modular design, SGH technologies can allow not only purification and use of natural gas produced from conventional reservoirs but also enable the exploitation of the potential stranded and discrete gas resources such as biogas, flue, and shale gases [13–15]. Moving toward the hydrogen economy, storing methane (25% hydrogen by weight) in the safe and compact solid form can be comparable to liquid ammonia (17.6% hydrogen by weight) especially when it is accompanied by proper carbon capture and sequestration or pyrolysis [1, 16]. However, the industrial application of such green material is hindered by stochastic and slow kinetics and high pressures required for hydrate formation [17]. Among the most efficient solutions to overcome the above challenges are using kinetic hydrate promoters (KHPs) and innovative reactor design.

Surfactants such as sodium dodecyl sulfate (SDS) are the most common KHPs employed to accelerate methane-tetrahydrofuran (THF) double hydrate [18–20]. Unfortunately, the process suffers from foam formation, which reduces methane uptake, prevents further scale-up, and creates the need for more effective promoters [21–23]. Recently, porous materials and amino acids were investigated as green KHPs to replace surfactants.

Porous materials such as zeolites, metal-organic frameworks, activated carbon, and others have been proven effective as KHPs [24–26]. They accelerate the kinetics by providing nucleation sites [27–29] for additional gas-liquid contact surfaces [30–32]. Zeolites are environmental-friendly materials with low cost, high stability, large surface area, tunable chemical properties, and above all insensitive to aqueous medium compared to other porous material such as metal-organic frameworks [33, 34].

Despite the advantages mentioned above, only a few studies investigated their performance as KHPs. To illustrate, zeolite Na-X (FAU-type) showed superior kinetic promotion in comparison over zeolites 3A and 5A (LTA-type). However, SDS was added [35, 36] as a co-promoter to achieve acceptable conditions [37, 38]. In a combined computational and experimental investigation, Omran *et al.* showed that acidic zeolite (H-Y, FAU-type) exhibited better kinetic promoting performance than the basic one 13X at a pressure 6 MP in absence of SDS. The improved performance is because the acidic form of the zeolite does not contain alkali metals that have a negative effect on hydrate nucleation [39, 40]. The acidic strength of the zeolite is also important [41]. For instance, Denning *et al.* showed that the confinement effect and surface properties of hydrophobic SSZ-13 (CHA-type) showed a higher promoting effect than SAPO-34 of the same chabazite topology in terms of water-to-hydrate conversion when they were used at low water to zeolite mass ratios (R_w=0.3-1.2) [42]. More recently, our group compared the performance of H-form ultrastable Y zeolite (H-USY) in different Si/Al ratios on hydrate formation from seawater at ambient temperature. The results confirmed the superior performance of more acidic and hydrophobic zeolites compared to their hydrophilic counterparts paving the way for their use on a larger scale [43]. Amino acids are also claimed to promising green hydrate promoters [44, 45]. Tryptophan and methionine, for example, have been reported to perform better as KHP for the formation of methane hydrates than hydrophilic amino acids like glycine [43, 46, 47]. On the other hand, some amino acids were reported as kinetic hydrate inhibitors, perturbing the local water arrangement [48–50]. The current difficulty of correlating amino acids hydropathy scale with their promotion or inhibition effect in research requires combining molecular simulation and experimental studies to understand their interaction mechanism with hydrate systems [51].

In addition to KHPs, different reactor designs can play an important role in enhancing the methane-THF double hydrate kinetics. Fixed bed reactors FBRs showed better hydrate kinetics and gas uptake than both NSR and stirred reactor configurations [52–54]. The FBR design shares the same configuration as the NSR with the packing materials lying at the bottom of the reactor [55]. A common advantage of different packing media, such as porous materials, glass beads, and metallic packing, is the enhancement of gas-liquid

contact surface area and the elimination of energy-intensive agitation [56]. However, the type of packing is also an important factor. For example, Babu *et al.* revealed that silica sand showed superior hydrate formation kinetics compared to silica gel, polyurethane foam packing, and stirred reactor configuration [57]. Another study by Kumar and Kumar showed that FBR with structured stainless-steel packing outperformed silica sand and the stirred reactor [58]. More recent studies with other metallic packing types and shapes such as copper foam, aluminum foam and, stainless-steel beads, confirmed the promoting role of metallic packing for hydrate growth [59–61]. This promoting effect can be attributed to the enhanced thermal conductivity and the increased surface and confinement effect in the case of dense packing. However, current research studies revealed three main limitations of metallic packing in hydrate formation. First, it has a relatively high density which reduces the gravimetric capacity of the system and limit its potential for scale-up. To illustrate, SS-316 has a density of $\sim$ 8000 kg/m^3, which is about 5 times higher than that of sand (1520-1680 kg/m^3) [62, 63]. Thus, a proper trade-off between the kinetic advantages and maintaining the gravimetric storage captivity is needed. The second drawback is related to the ineffective arrangement of the metallic packing inside the reactor. We have found that the vast majority of these studies the heavy metallic packing itself rests at the bottom of the reactor [58, 59]. This arrangement of the packing provide only the advantage of good heat transfer for a small part of the reaction system. More precisely, the important area of gas-liquid interface, most of the liquid phase and all the gas phase [57, 64]. Finally, most of the research studies that involved have to further SDS to enhance the kinetic toward an acceptable range due to the lack ineffective arrangement of the material packing at the reactor [59, 64]. This use of SDS has many drawbacks as foaming, loss of storage capacity and erratic instrument measurement due the two phases [65].

While SGH technology has many advantages, finding the optimum storage conditions in the context of the so-called "self-preservation" phenomena is an important step toward feasible energy storage process. Below the freezing point of water, this phenomena describes the unexpected prolonged stability of gas hydrates outside their thermodynamic stability zone. While "self-preservation" is widely observed in a temperature range of 240-273 K [66], it was found that pure methane hydrate stored at 253 K exhibited high stability as it is become surrounded by an ice layer [67, 68]. Similar observations were demonstrated for hydrates of natural gas mixture and THF-CH_4 binary hydrates [66, 69]. Optimizing the medium and long-term methane storage conditions in gas hydrates as an alternative energy storage can have practical and direct implications on problems such as the current EU energy crisis. To illustrate, the current combined natural gas storage facilities in the EU are not enough to ensure the energy security during the four months of winter. In particular, the total underground storage capacity is about 100 billion cubic

metres while consumption was around 400 billion cubic metres in 2020 according to the official estimations [70].

The primary objective of this study is to enhance the formation kinetics of CH_4-THF hydrates using an acidic zeolite (H-form SSZ-13 zeolite (H-SSZ-13)) and different biodegradable amino acids (L-leucine, L-methionine, and L-tryptophan) as an alternative green KHPs to replace synthetic surfactants such SDS. The promoting mechanism of these eco-friendly KHPs is studied by combining density functional theory (DFT) calculations and detailed experimental kinetic data. Then, we use an engineering approach that combines those environmentally benign promoters with innovative reactor design with metallic filament packing to maximize the hydrate growth kinetics. Finally, we explored boosting economic feasibility by increasing the temperature toward near ambient (293.15 K) and tested the long-term storage at 253.15 K and ambient pressure for medium and long-term storage and specified its implications on hydrate technology.

2. Materials and Methods

2.1. Materials and Experimental Procedure

Methane gas (99.99% purity) was acquired from Linde, NH_4-SSZ-13 was purchased from ACS Materials (USA) and Tetrahydrofuran (THF, AR grade 99.99%) from Alfa Aesar. The NH_4-form of zeolite was calcined ~~was~~ at 450°C for 4 hours to obtain the acidic form (H-SSZ-13). Amino acids L-tryptophan (reagent grade, 99 %), L-leucine (reagent grade, 99%), L-methionine (reagent grade, 99%), and glycine (reagent grade, 99%) were purchased from Alfa Aesar. A volumetric flask was used to prepare the blank THF 5.56 mol% solution or its mix with 300 ppm of zeolite or amino acid and where solutions were mixed for 15 mins.

The instrument used for hydrate formation and dissociation is schematically described in **Fig.S1** and details of the set-up are provided in previous studies [39, 43]. In brief, it is composed of a 450 cm^3 high-pressure stainless-steel (SS-316) reactor (CR; Parr) that is equipped with light-weight corrosion-resistant MFP. The morphology and detailed elemental composition of MFP is shown in **Table S1**, and **Fig.S2**. To ensure data consistency, each experiment was repeated at least three times, ~~as~~ and the average values reported in **Tables S2-S7**. All experiment has been performed under isochoric and isothermal conditions. A detailed description of hydrate formation and recovery experiments and calculations is reported in supporting information as described in **Sections S2.1 and S2.2**. For the storage procedure, the reactor content was quenched to liquid nitrogen temperature and then recovered under liquid nitrogen in an external closed stainless steel container which was

preserved in a refrigerator under 253.15 K and atmospheric pressure. Periodically, the sample weight has been followed to check the methane loss.

2.2. Characterization of H-SSZ-13 and Binary CH_4-THF Hydrate

The calcined acidic zeolite (H-SSZ-13) underwent comprehensive characterization utilizing a range of techniques to gain insights into its properties. Scanning electron microscopy (SEM) provided visual information about its morphology and surface features. Powder X-ray diffraction (PXRD) analysis was employed to determine its crystal structure and phase purity. Inductively coupled-atomic plasma emission spectroscopy (ICP) analysis allowed for the quantification of elemental composition, while energy dispersive X-ray (EDX) provided further elemental mapping and identification. N_2 adsorption measurements were performed to assess the zeolite's surface area, pore size distribution, and porosity. These characterization techniques collectively offered a comprehensive understanding of the H-SSZ-13 zeolite as outlined in **Section S3.1**. For the synthesized binary CH_4-THF hydrate, a similar approach was taken to unravel its structural and chemical properties. PXRD analysis was employed to confirm the formation of the hydrate phase and to investigate its crystal structure. Raman spectroscopy was utilized to probe the vibrational modes of the hydrate, providing insights into its molecular arrangement and interactions. Additionally, ^{13}C nuclear magnetic resonance spectroscopy was employed to study the carbon environment within the hydrate structure. These characterization techniques, detailed in **Section S3.2** of the supporting information, played a crucial role in elucidating the key characteristics of the CH_4-THF hydrate system.

2.3. Density Functional Theory Calculations

For the computational part, we used DFT calculations [71, 72]. We used projected augmented wave method as implemented in Quantum Espresso software [73]. This method offer significant technical and practical advantages in identifying clathrate hydrate promoters [12]. One of the benefits of employing density functional theory in contrast to classical molecular dynamics (MD) is the absence of reliance on empirical interatomic potentials [74]. DFT simulations, often termed first-principles calculations, provide a reliable and accurate description of materials without the need for adjustable parameters. This makes DFT particularly valuable in the study of kinetic hydrate promoters, where precise understanding of the underlying mechanisms is crucial. Furthermore, the ability to validate DFT predictions with experimental data enhances its practical utility [43, 75]. By comparing calculated results with observed outcomes, the reliability and accuracy of DFT can be assessed, boosting confidence in its use for identifying clathrate hydrate promoters. A full detailed description of the promoter-hydrate models and calculation parameters are shown in supporting information **Section S4**.

3. Results and discussion

The characterization of H-SSZ-13 included PXRD to study the crystal structure and identify phase purity. As depicted in **Fig.S3**, the obtained diffraction pattern clearly demonstrates the characteristic peaks corresponding to the H-SSZ-13 zeolite. SEM was employed to investigate the morphology and surface features of the zeolite. **Fig. S4** showcases the micrograph from SEM, revealing the particle size distribution and the presence of well-defined crystalline structures. All data shows that the employed material is highly crystalline. ICP and EDX revealed that Si/Al ratio of 9. Finally, **Table S10** presents the N_2 physisorption measurements conducted to assess the porosity and specific surface area of the H-SSZ-13 zeolite.

PXRD analysis confirmed sII formation, which coexists with a small amount of hexagonal ice. Raman spectroscopy analysis on the synthesized binary hydrate was also performed. The spectroscopic data revealed methane occupancy in 5^{12} small cage of sII by a sharp peak at $\sim$ 2911.1 cm^{-1} [76]. ^{13}C nuclear magnetic resonance measurements confirmed the Raman result with methane occupancy in 5^{12} small cages of sII by the sharp peak at -4.3 ppm. As expected, THF occupy the large cages as indicated by the double peaks at 26.1 and 69.2 ppm as illustrated in **Fig.S5** [43]. More details about the characterization techniques and results are provided in supporting information.

3.1. Prediction of Amino Acids Hydrate Promoting Effect at Molecular Level

DFT calculation has been successfully used to report different promoters [39, 43] or inhibitors effect on hydrate formation [77, 78]. In our previous studies, we have utilized first principle calculations to explain the promoting effect of acidic and hydrophobic zeolites, which can be applied in the case of H-SSZ-13. Here, we have studied s different amino acids to anticipate their promoting effect as KHPs. First, the molecular level investigation aimed to find the best exchange-correlation functional representing the methane hydrate 5^{12} cage and then the hydrate-amino acids system. Then, the optimum exchange-correlation functional was employed to analyze amino acids-hydrate interactions which are dominated by H-bonding and van der Waals dispersion forces. Clathrate stability is dependent on the host-guest interaction[79] which can be evaluated through the interaction energy host-guest interaction energy (ΔE^{HG}) , as detailed in our previous study [43].

The host-guest interaction energy of methane in the 5^{12} cage was calculated with the use four different exchange-correlation functionals. Using revPBE, the calculation of binding energy resulted in +2.3 kJ/mol failing to determine the host-guest interactions accurately. Thus, we tested rVV-10, vdW-DF2, and SCAN-rvv10 exchange-correlation functionals to capture the van der Waals dispersion forces, as shown in **Fig.S8**. Compared

to -32.55 kJ/mol obtained by MP2/6-311++G(d,p) [79], the interaction energy value of -27.78 kJ/mol obtained from vdW-DF2 shows close result to the accurate MP2 calculations compared to the others. After confirming the calculation accuracy on the $CH_4@5^{12}$ cage, we studied the interaction of amino acid molecules with the hydrate cage.To benchmark the promoting effect, we compare the interaction of different amino acids with $CH_4@5^{12}$ cage to that of a single water molecule with the same cage.

Based on the interaction energy of calculation, L-tryptophan showed the lowest interaction energy with -49.49 kJ/mol compared to L-methionine and L-leucine, which showed -58.03, and -52.99 kJ/mol, respectively. The more negative interaction energy indicates a more inhibitory effect for the amino acid. Accordingly, the promoting effect of amino acids is expected to be L-tryptophan $>$ L-leucine $>$ L-methionine as illustrated in **Fig.1**. To further confirm, we did the same calculation on glycine [48, 50], an amino acid known for its inhibiting effect on hydrate formation [49, 80], and the resulting interaction energy was -74.64 kJ/mol. This value is significantly lower than all the other promoters in the study. The optimized amino-cage L-tryptophan and glycine are shown in **Fig.2**.

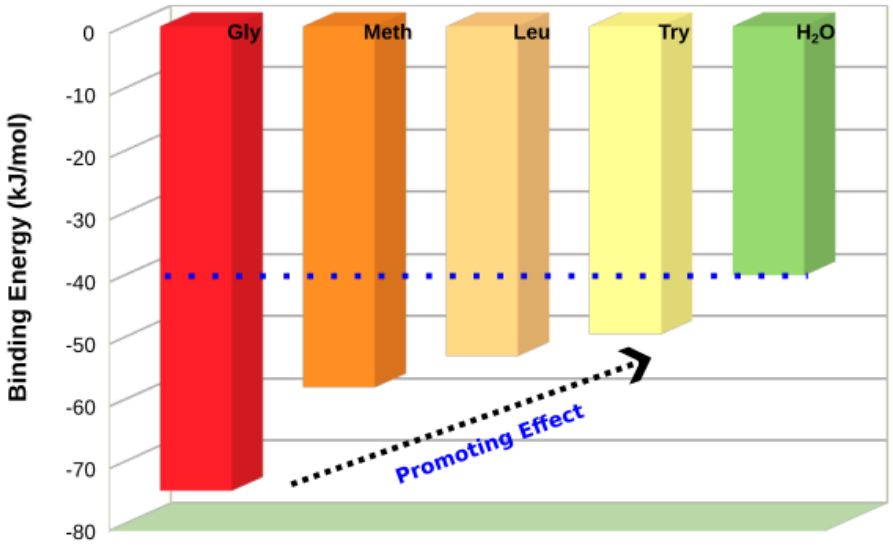

Figure 1: Comparison of binding energy (kJ/mol) of several amino acids to the (5^{12}) small methane cage compared to the interaction with H_2O. Higher binding energy shows that the amino acid disturbs the cage formation and acts as an inhibitor and *vice versa*, which agrees well with experimental observations [81–84].

The research in this study shows that the hydate promoting effect of amino acids does not only depend on their hydrophobicity alone but also on interactions with hydrate cage

(e.g., hydrogen bonding) and thermodynamic conditions. To illustrate, while the most hydrophobic amino acids L-tryptophan showed the highest promoting effect among amino acids in all temperatures, L-leucine did not always show a more promoting effect than L-methionine despite its higher hydrophobicity according to Kyte and Doolittle scale [85, 86].

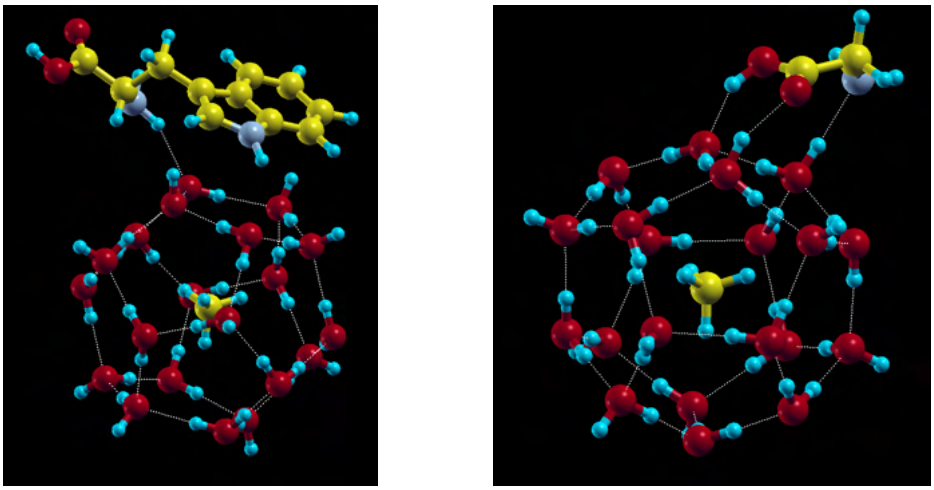

(a) (b)

Figure 2: Optimized configurations of small (5^{12}) cage with amino acids (a) L-tryptophan and (b) glycine. Nitrogen, hydrogen, carbon, and oxygen atoms are shown in violet, blue, yellow, and red colors, respectively.

3.2. Effect of Promoters on Binary CH_4-THF Hydrate Formation

To validate the outcome of first principle calculations from **Section 3.1**, we compared the performance of different amino acids in the NSR in the first set of experiments. At 283.15 K, the blank solution needed an induction time of 181.33 min. Adding 300 ppm of H-SSZ-13 has reduced the average induction time to about 11 min, while the average t_{90} (time taken for 90% completion of methane uptake) of 286.2 min outperformed other amino acids promoters, as shown in **Fig.3**. The presence of H-SSZ-13 has provided further liquid gas contact area and provided nucleation sites for hydrate formation. In the absence of extraframework cation as explained in the introduction, the acidity of H-SSZ-13 can increase gas insertion and improve the gas diffusion coefficient by increasing sII flexibility, similar to acidic additives such as perchloric acid ($HClO_4$) [87, 88]. This conclusion agrees well with our previous studies where the acidic forms of USY and Y zeolites were employed. It is also confirmed by a recent study revealing that zeolite acidity is comparable to those of superacids [89]. Furthermore, the presence of acidic zeolite granted heterogeneous nucleation through the whole aqueous bulk solution, as will be detailed in

the next section.

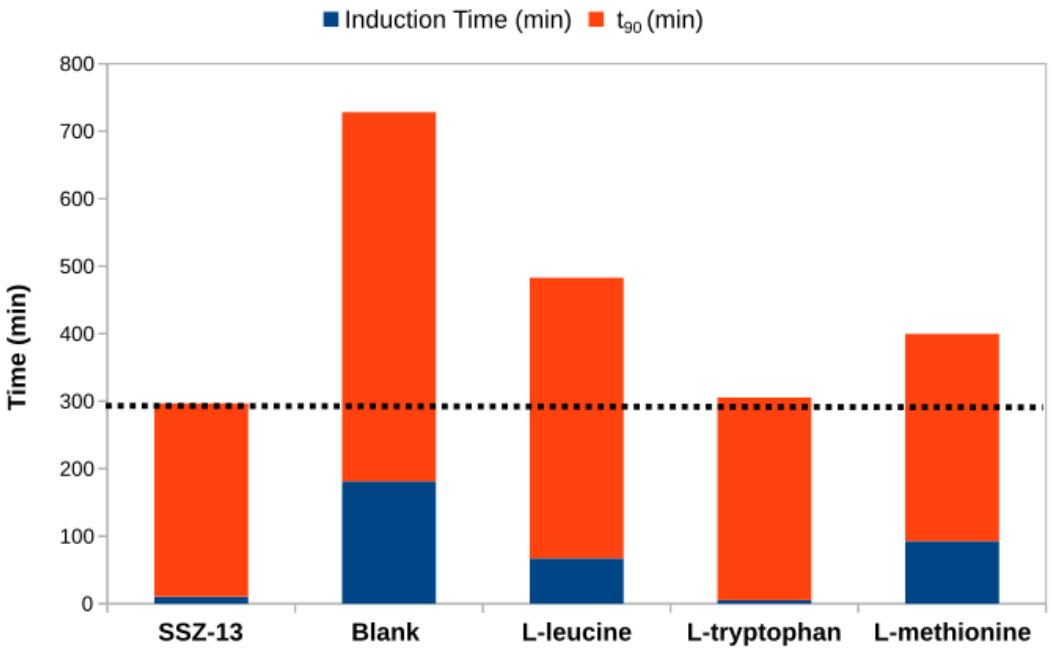

Figure 3: Comparison of the average induction time and t_{90} of 300 ppm H-SSZ-13 and different amino acids at 6 MPa and 283.15K

On the other hand, among the amino acids used, the hydrophobic L-tryptophan reduced the induction time significantly to 5.2 min compared to 67.3 min for L-leucine and 92.8 min for L-methionine, which agrees well with our computational expectations. When it comes to gas uptake, H-SSZ showed the highest gas uptake of 115.82 mmol gas/mol H_2O compared to the best amino acids reported at that temperature (L-tryptophan), which showed 109.3 mmol gas/mol H_2O. This difference comes from the fact that although the amino acids increase the initial gas solubility into the THF solution, they still can slightly disturb the hydrate formation in a later stage by hydrogen bonding to the cage with both the amino group and secondary amine group. On the other hand, the H-SSZ-13 enhances the nucleation step by acting as heterogeneous nucleation sites. The enhanced kinetics uptake was also accompanied by almost full recovery (95-99 %) of the methane by slight heating up indicating a reversible process.

Increasing the temperature to 288.15 K and to near ambient (293.15K),has resulted in

raised induction time and decreased gas uptake. Such behavior is a consequence of the exothermic nature of clathrate formation. **Fig.4** shows the gas uptake of different promoters at 293.15 K. However, one can also notice that t_{90} is at its highest at 288.15 and goes down at 293.15 K as shown in **Table S2** and **Table S3**. While the increase of t_{90} at 288.15 K compared to 283.15 K can be justified by the slower kinetics, the lower t_{90} at 293.15 K indicates that the reaction is stopped at an earlier premature stage and accompanied by lower gas uptake. The latter can be explained by water's poor heat conductivity, which has the double role of being a reactant and a cooling medium. Another important observation is that increasing the temperature, L-tryptophan showed better kinetic performance in terms of induction time and gas uptake compared to other promoters, as shown in **Fig.4**. At the relative temperature and poor thermal conductivity, gas dissolution in the aqueous medium is the determining factor for kinetics. The poor performance of H-SSZ-13 at that temperature, despite the relatively short induction time, can be explained by its need for a certain critical concentration of dissolved methane to be able to trigger their role as nucleation sites. Finally, we tested the addition of 300 ppm of glycine to the THF solution. No gas uptake was observed after 24 h revealing glycine's inhibiting effect, which agrees well with previous experimental results and our DFT calculations.

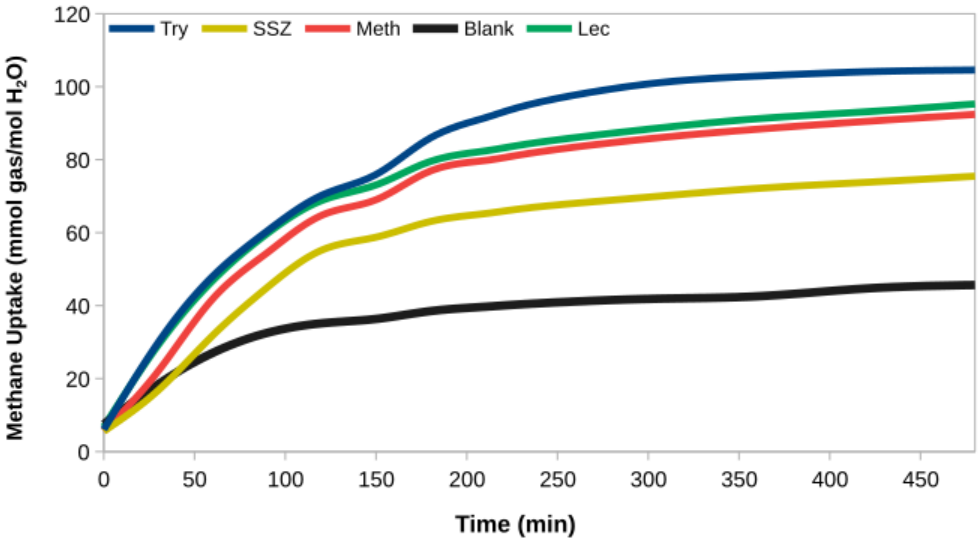

Figure 4: Comparison of methane uptake (mmol gas/mol H_2O)in the presence of 300 ppm H-SSZ-13 and different amino acids at 6 MPa and 293.15K.

3.3. Effect of Modified Reactor Design on Binary CH_4-THF Hydrate Formation

As it has been shown in **Section 3.2**, performing the hydrate synthesis in the traditional NSR showed a high t_{90}, especially when increasing the temperature near ambient conditions to meet the economic requirements. The slow hydrate nucleation can be attributed to low gas-liquid heat transfer, and reactor design in terms of shape and cooling, i.e., the radial gradient of temperature. To illustrate, one can see that hydrate formation is more around the reactor wall due to the cooling around, which resulted in heat dissipation to the nearby aqueous solution **Fig.5a**.The poor heat transfer results in less hydrate formation when moving toward the center, with a clear advantage of H-SSZ-13 over amino acids (see below **Fig.5**).

However, even in the case of zeolites which allowed heterogeneous nucleation, the formation of thin hydrate film at the surface hinders further gas-liquid mass transfer. Thus, we have utilized a light-weight metallic filaments network with a rough surface with the following objectives: (1) increase the heat conductivity, (2) break the hydrate thin film into smaller sections, (3) provide larger liquid-gas contact on the rough metal surface, and (4) extend the heat conduction to the gas phase. **Fig.5** shows the features of hydrates formed in the NSR in the presence of L-methionine (**Fig.5a**), H-SSZ-13 (**Fig.5a**), and those formed in FBR in presence of H-SSZ-13 (**Fig.5c**) . The zeolite improved the hydrate formation in bulk compared to L-methionine, while the presence of intervened filaments allowed exploiting the full potential of reactor volume compared to NSR. Moreover, the MFP has ruptured the hydrate thin film allowing better diffusive mass transfer and gas-liquid contact as illustrated in **Fig.5c** and **Fig.6** .

(a) (b) (c)

Figure 5: Hydrate formation at 6 MPa and 293.15 K at (a) L-methionine at NSR (b) H-SSZ-13 at NSR and (c) H-SS13 at FBR.

At the near-ambient temperature of 293.15 K as shown in **Table S5**, we have found that the average induction time for a blank solution is about 81.7 min, indicating that the FBR is reduced by 110% compared to NSR configuration. Moreover, the utilization of

promoters in the new FBR configuration has reduced the reaction time t_{90} to less than 3 hours which is feasible from both technical and economic points of view. Improving the thermal conductivity, H-SSZ-13 showed the best kinetic performance among the studied promoters with a significant simultaneous reduction in induction time to only 2.7 min (compared to 58.2 min in NSR) and the highest gas volumetric capacity of 104.5 V/V as shown in **Fig.7**.

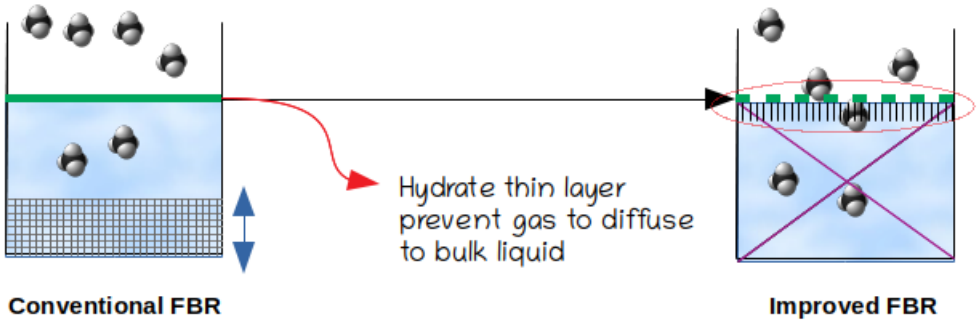

Figure 6: Illustration of metallic packing in hydrate FBR and the improved FBR presented in this study.

These results point out that packing inside the reactor has successfully modified the surface properties and increased the gas mass transfer to a sufficient concentration to enhance the nucleations with acidic zeolites at the earlier stages. Moreover, it brokes the hydrate film formed early in the reaction and thus maintained suitable gas diffusion into the bulk medium. Among the amino acids, L-tryptophan slightly outperformed performed L-leucine in terms of both t_{90} and induction time but with a clear advantage of gas uptake and volumetric storage capacity of 103.73 mmol gas/mol H_2O and 103.11 V/V, respectively. Despite showing the lowest kinetic performance among the studied promoters, L-methionine in FBR still significantly reduced induction time to only 5 mins compared to 83.6 min when it was used in NSR configuration. This promoting performance of different amino acids in the case of FBR agreed well with our DFT calculation results. **Fig.8** compares the induction time and gas uptake published in the other studies at the same thermodynamic conditions. It shows that the kinetic performance and gas uptake of H-SSZ-13 and L-tryptophan outperformed hollow silica and SDS at the same temperature of 293.15 K and 6 MPa [35]. Moreover, it could get almost the same gas uptake at a higher pressure of 8 MPa with about 25 times reduction of induction time [90].

Decreasing the temperature from 288.15 to 283.15 shown in **Table S6 and Table S7**, resulted in a decrease in both induction time and t_{90}. Moreover, the kinetic performance

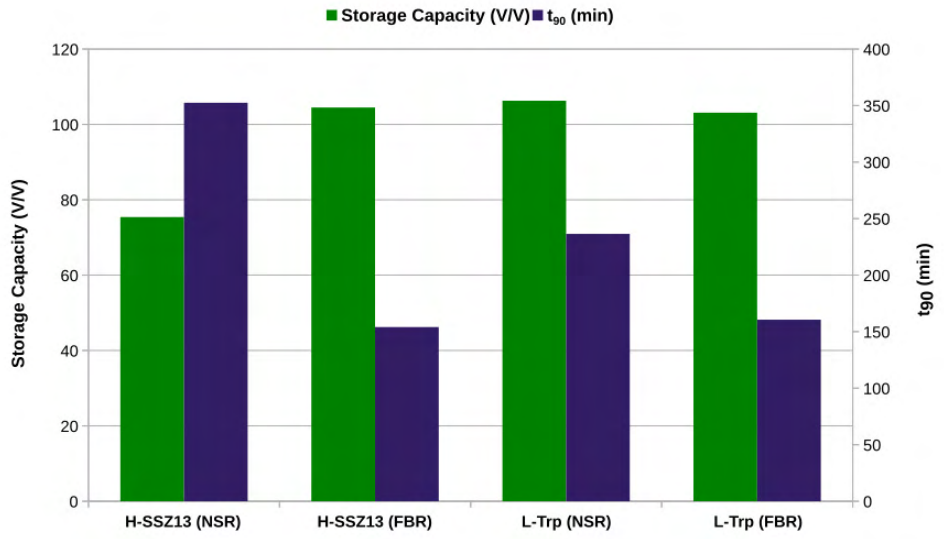

Figure 7: Comparison of storage capacity and t_{90} of 300 ppm H-SSZ-13 and L-tryptophan for hydrate synthesis in NSR and FBR at 6 MPa and 293.15K

of all promoters at those temperatures outperformed those under NSR conditions. To illustrate, H-SSZ-13 resulted in a volumetric capacity of 114 V/V at 288.15 K, with an increase of 42.7% compared to NSR under the same conditions. At the same temperature, L-tryptophane resulted in a gas uptake of 115.4 mmol gas/mol H_2O, which is 22.6% higher than the same conditions at NSR. Lowering the temperature to 283.15K significantly accelerated the reaction kinetics and reduced the t_{90} to less than 80 mins. For example, there was almost instantaneous gas uptake in the case of both H-SSZ-13 and L-tryptophan. Despite the fast reaction compared to NSR and the higher temperature, H-SSZ-13 and L-tryptophan and reached an impressive volumetric capacity (110.7-117.0 mmol gas/mol H_2O). As shown in **Fig.9**, such outstanding performance is due to the enhanced kinetic and heat transfer that resulted in a sharper temperature peak. We believe that both kinetics and good heat transfer are interconnected and the presence of good heat transfer surface can enhance the formation kinetics. One clear evidence is shown at **Fig.5(a)**, where the hydrate is formed on the reactor wall (good heat conductor) rather in the middle of the reactor where water only exists which is a reflection of the expected heat transfer gradient. This evidence is in agreement with previous experimental observations [91].

3.4. Techno-economic Aspects Implications and Long-Term Storage

One of the main goals of this study is to connect molecular-level investigation and macro-kinetic studies to the engineering and technological aspects. Establishing this con-

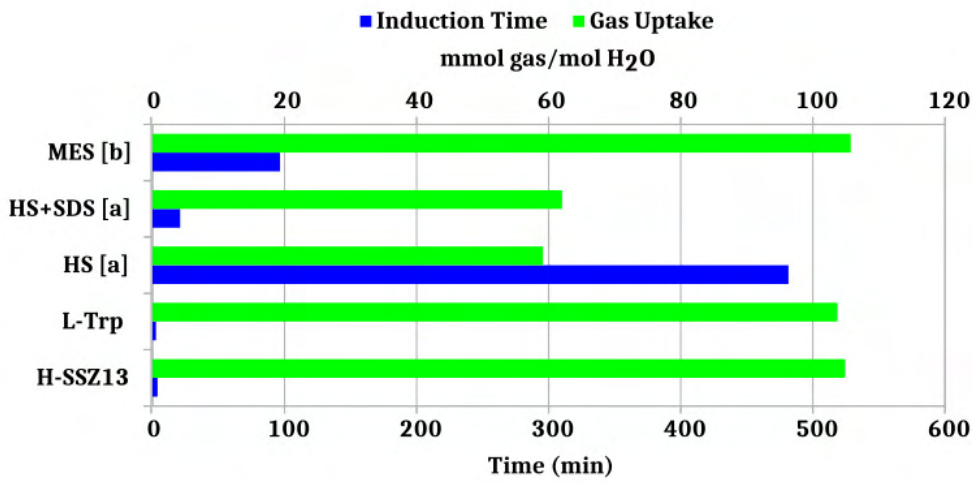

Figure 8: Comparison of the average induction time and methane uptake of this work with other studies **[a]** using hollow silica (HS) and (HS+SDS) at 6 MPa and 293.15K [35] and **[b]** using methyl ester sulfonate (MES) at 8 MPa and 293.15 K [90].

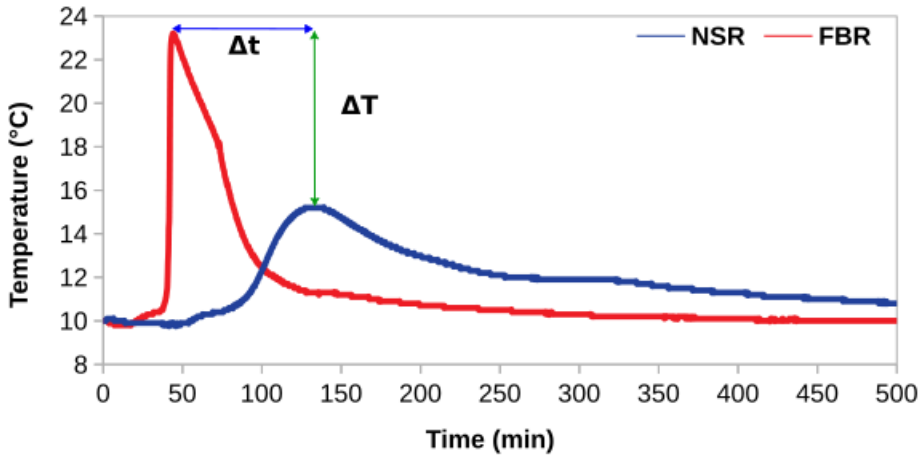

Figure 9: Comparison of temperature profiles of hydrate formation in NSR and FBR at 6 MPa and 283.15K.

nection at the early research stage will guarantee the smooth and economic scale-up process of SGH. In this section, we explain the possible economic outcome of this study's technological choices, such as realistic conditions (near-ambient temperature) and a moderate pressure of 6 MPa, the use of FBR, and the selection of low-cost green promoters to

boost the hydrate formation process kinetics. Then, we show the importance and possibility of using SGH technology for long-term storage compared to other technologies such as CNG and LNG. Finally, we discuss some perspectives on this research.

It is important to reduce the cost of the hydrate formation process to cut the overall operating cost. We performed a preliminary economic analysis based on the key parameters that reflects the cost : storage thermodynamic requirements (P,T), stability, and storage time. According to Veluswamy *et al.*, the capital expenditure over operating expenditure ratio in the case of sII is 4.6 compared to 5.3 in the case of CNG with the same volumetric capacity (115 V/V) [92]. Although there is a clear advantage of SGH in terms of safety and long-term storage economics [93], this ratio still reflects the high cost of hydrate synthesis. Lucia *et al.* estimated that the compression cost is about 70-80 % of the total cost for methane hydrate synthesis in a large-scale 25 L reactor [94]. Thus, we have utilized THF as a thermodynamic promoter to relax the P-T conditions to 6 MPa and 293.15 K, significantly boosting the process economics [95].

The role of THF is not only limited to reducing the thermodynamic requirements but also extended to increase the stability of sII clathrate. The stability of binary CH_4-THF sII clathrate is higher than pure THF clathrate, as revealed by high-pressure differential scanning calorimetry analysis [96]. The high stability allowed storing CH_4-THF pellets at 1.5 atm and 271.5 K for 2 months. In this study, the CH_4-THF hydrates were transferred under liquid nitrogen without further processing to a container and could be stored for 8 months at 253.15 K and atmospheric pressure. During that period, the hydrate sample weight loss did not exceed 0.6 wt% for 4 months and 2.5 wt% over 8 months from about 8.35 wt% of the stored methane as shown in **Fig.10**. The possibility of storing methane at atmospheric or slightly positive pressure is a clear advantage when it comes to long-term storage compared to LNG which requires extensive refrigeration to keep LNG at 113 K which is estimated to be typically **27%** of the cost or 32.4 euros per gigawatt-hour per day (€/GWh/d) (0.5 €/t LNG/day) as per current gas prices [97]. Due to boil-off gases, LNG can suffer from 0.05 wt% loss per day in LNG or 2-6 wt% loss in cargo depending on the voyage length, typically 3 weeks [98].

Thus, the loss in long-term storage can be approximately 12 wt% over 4 months in the best cases. Based on our experimental results, methane storage at the synthesized hydrate without further processing can be more economically attractive than a typical LNG tank. As illustrated in **Fig.11**, SGH from our experiments showed a significantly lower methane loss compared to a typical LNG tank for at least for months considering the best cases of boil-off losses [98]. After 8 months, the methane loss in the LNG is estimated to be-

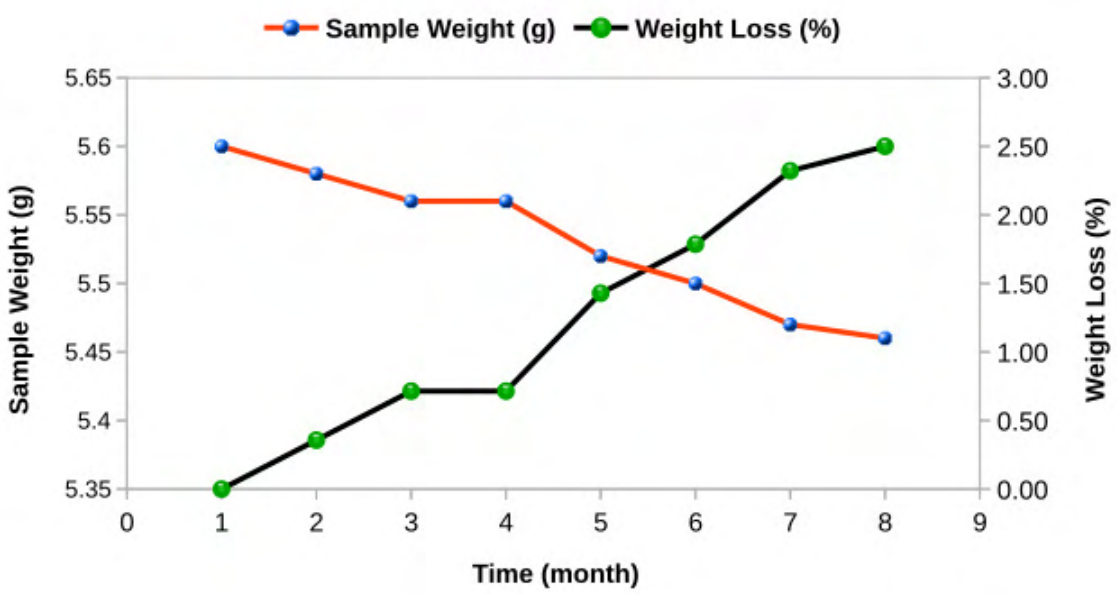

Figure 10: Evolution of average weight loss ($\pm$ 0.03 %) of CH_4-THF hydrate stored in 253.15 K over 8 months.

come slightly lower compared to our SGH. Nevertheless, the storage of SGH is still much more advantageous due to the large difference between refrigeration requirements of LNG transportation and storage at 113 K (47% of LNG total cost) compared to those required for SGH at 253 K [11, 97]. Further optimization and detailed more detailed economic evaluation is required to treat other factors.

Finally, we have used an innovative green approach that combined green KHP and improved FBR design. Our packing is less than 0.08 wt/wt of the hydrate content, which is significantly lower compared to different packing reported in other research studies. For example, Kumar *et al.* reported weight percentages of (0.28-1.2) for traditional stainless steel packing (SSP), 1.1 for silica gel, and even 5.0 for silica sand [99] . While this study compared FBR to NSR, here we address the economical aspects of using stirred reactors, which are the most common reactor configuration to increase the gas-liquid contact, enhance mass transfer, and shorten the induction time [100, 101]. In fact, the mass transfer in those reactors drops quickly after the nucleation as a widely used bottom-mounted laboratory magnetic stirrer does not affect the floating hydrate clusters that arrange themselves in a thin layer preventing further gas-liquid contact [102]. A number of scale-up studies have shown that the top-mounted stirrer design is more efficient than the stirred reactor

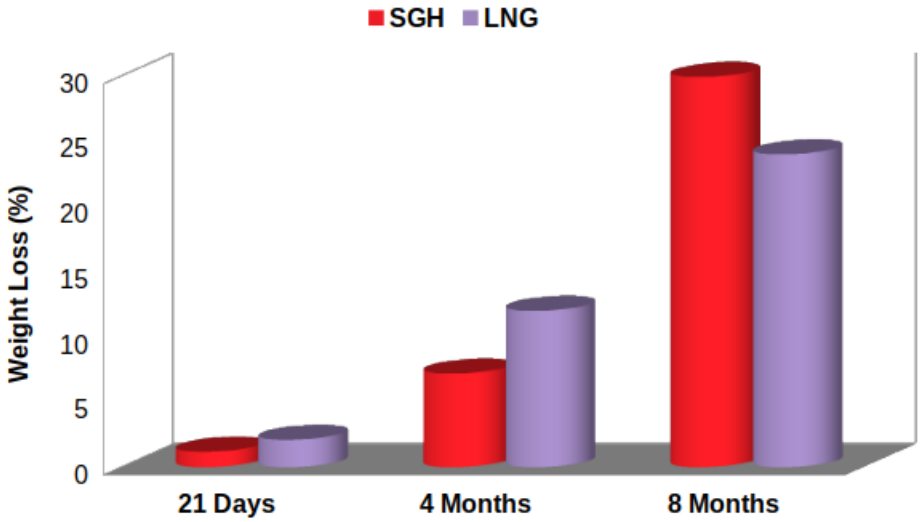

Figure 11: Comparison of gas weight loss for CH_4-THF hydrate stored in 253.15 K and LNG in 113 K over 8 months.

configuration [103], however, due to its higher cost it has not been adopted commercially [104]. Namely, the lower hydrate weight in water ($\leq$ 5 wt%) results in post-processing filtration cost and increasing agitation energy demand as the slurry thickens [105, 106]. Thus, compared to both stirred and non-stirred configurations, the improved FBR design with light-weight packing showed superior performance. This research also showed that gas hydrates can maintain 90-117 V/V of methane hydrate stored for at least 4 months -or a full winter season- without significant loss compared to LNG in a much lower thermodynamic requirements. Based on the above results, the perspective studies will include surveying more computationally designed green promoters, experimental studies on more acidic zeolites, and amino acids. Further improvements in the reactor design to increase the surface area of liquid-gas contact and exploring different hydrate structures is expected to enhance the storage capacity.

4. Conclusions

This work provides an integrated approach for storing methane as an energy vector in hydrates combining environmentally benign KHPs, namely acidic zeolites and amino acids, and innovative reactor design to accelerate reaction kinetics and improve the storage capacity. It also provides a first-principle methodology to evaluate the promoting efficiency of amino acid zeolite. Another important issue addressed in the study is the

long-term storage in SGH compared with state-of-the-art LNG technology.

Different zeolite and amino acids KHPs at low concentrations of 300 ppm were evaluated under 6 MP and at different temperatures in a NSR. H-SSZ-13 showed the best performance at 283 K with an average induction time of 10.5 mins, hydrate volumetric capacity of 115 V/V, and recovery of 97%. The L-tryptophane outperformed other KHPs at 283 K and 288 K in terms of induction time and gas uptake. However, the performance of all promoters dropped at 293.15 K due to low methane solubility and mass transfer limitations.

~~We~~ The study introduced a FBR equipped with special MFP to overcome the above limitations. The new MFP-FBR improved mass and heat transfer by increasing the thermal conductivity and breaking the hydrate thin film formation without significantly affecting the gravimetric storage capacity.The experimental data showed that the presence of the green KHP H-SSZ-13 significantly reduced the reaction time and increased the volumetric storage capacity to 96% of the theoretical value. The overall performance of amino acids followed the order of L-tryptophan $>$ L-leucine $>$ L-methionine, which agreed well with ~~our~~ the binding energy value obtained from first-principle calculations. Finally, this research demonstrated the potential of SGH for long-term methane storage in economic conditions compared to LNG which can have practical implications on the future energy storage in the EU. Future research points will include comparative life cycle analysis of both SGH and LNG and the minimization of the use of solvent thermodynamic promoter.

Appendix A. Supplementary data

Supplementary data to this work can be found online at (*link to be provided*).

Acknowledgments

The authors thank CRIANN (Centre Régional Informatique et d'Applications Numériques de Normandie) Normandy, France for providing the computing resources and the (ANR-17-CHIN-0005-01) grant for financial support. The authors also thank Cassandra Vion for her contribution in the graphical abstract.

References

[1] A. Omran, N. Nesterenko, V. Valtchev, Zeolitic ice: A route toward net zero emissions, Renew. Sustain. Energy Rev. 168 (112768) (2022). doi:10.1016/j.rser.2022.112768.

[2] R. Hafezi, A. N. Akhavan, S. Pakseresht, D. A. Wood, Global natural gas demand to 2025: A learning scenario development model, Energy 224 (2021) 120167. doi:10.1016/j.energy.2021.120167.

[3] A. Omran, S. H. Yoon, M. Khan, M. Ghouri, A. Chatla, N. Elbashir, Mechanistic insights for dry reforming of methane on Cu/Ni bimetallic catalysts: DFT-assisted microkinetic analysis for coke resistance, Catalysts 10 (9) (2020) 1–16. doi:10.3390/catal10091043.

[4] T. Klatzer, U. Bachhiesl, S. Wogrin, State-of-the-art expansion planning of integrated power, natural gas, and hydrogen systems, Int. J. Hydrogen Energy 47 (47) (2022) 20585–20603. doi:10.1016/j.ijhydene.2022.04.293.

[5] H. Song, Y. Liu, H. Bian, M. Shen, X. Lin, Energy, environment, and economic analyses on a novel hydrogen production method by electrified steam methane reforming with renewable energy accommodation, Energy Convers. Manag. 258 (January) (2022) 115513. doi:10.1016/j.enconman.2022.115513.

[6] A. Kumar, P. Singh, P. Raizada, C. M. Hussain, Impact of COVID-19 on greenhouse gases emissions: A critical review, Sci. Total Environ. 806 (2022) 150349. doi:10.1016/j.scitotenv.2021.150349.

[7] M. Sesini, S. Giarola, A. D. Hawkes, Solidarity measures: Assessment of strategic gas storage on EU regional risk groups natural gas supply resilience, Appl. Energy 308 (December 2021) (2022) 118356. doi:10.1016/j.apenergy.2021.118356.

[8] J. Javanmardi, K. Nasrifar, S. H. Najibi, M. Moshfeghian, Natural gas transportation: NGH or LNG?, World Rev. Sci. Technol. Sustain. Dev. 4 (2-3) (2007) 258–267. doi:10.1504/WRSTSD.2007.013585.

[9] Y. Yin, J. S. L. Lam, Bottlenecks of LNG supply chain in energy transition: A case study of China using system dynamics simulation, Energy 250 (2022) 123803. doi:10.1016/j.energy.2022.123803.

[10] T. T. Pedersen, E. K. Gøtske, A. Dvorak, G. B. Andresen, M. Victoria, Long-term implications of reduced gas imports on the decarbonization of the European energy system, Joule 6 (7) (2022) 1566–1580. doi:10.1016/j.joule.2022.06.023.

[11] H. P. Veluswamy, A. Kumar, Y. Seo, J. D. Lee, P. Linga, A review of solidified natural gas (SNG) technology for gas storage via clathrate hydrates, Appl. Energy 216 (February) (2018) 262–285. doi:10.1016/j.apenergy.2018.02.059.

[12] A. Omran, N. Nesterenko, V. Valtchev, Ab initio mechanistic insights into the stability, diffusion and storage capacity of sI clathrate hydrate containing hydrogen, Int. J. Hydrogen Energy 47 (13) (2022) 8419–8433. doi:10.1016/j.ijhydene.2021.12.186.

[13] J. S. GUDMUNDSSON, V. ANDERSSON, O. I. LEVIK, M. MORK, Hydrate Technology for Capturing Stranded Gas, Ann. N. Y. Acad. Sci. 912 (1) (2006) 403–410. doi:10.1111/j.1749-6632.2000.tb06794.x.

[14] Z. M. Xia, X. S. Li, Z. Y. Chen, G. Li, K. F. Yan, C. G. Xu, Q. N. Lv, J. Cai, Hydrate-based CO2 capture and CH4 purification from simulated biogas with synergic additives based on gas solvent, Appl. Energy 162 (2016) 1153–1159. doi:10.1016/j.apenergy.2015.02.016.

[15] F. Filarsky, C. Schmuck, H. J. Schultz, Development of a biogas production and purification process using promoted gas hydrate formation — A feasibility study, Chem. Eng. Res. Des. 134 (2018) 257–267. doi:10.1016/j.cherd.2018.04.009.

[16] S. Timmerberg, M. Kaltschmitt, M. Finkbeiner, Hydrogen and hydrogen-derived fuels through methane decomposition of natural gas – GHG emissions and costs, Energy Convers. Manag. X 7 (February) (2020) 100043. doi:10.1016/j.ecmx.2020.100043.

[17] B. P. Prajwal, K. G. Ayappa, Evaluating methane storage targets: From powder samples to onboard storage systems, Adsorption 20 (5-6) (2014) 769–776. doi:10.1007/s10450-014-9620-1.

[18] H. Najibi, M. Mirzaee Shayegan, H. Heidary, Experimental investigation of methane hydrate formation in the presence of copper oxide nanoparticles and SDS, J. Nat. Gas Sci. Eng. 23 (2015) 315–323. doi:10.1016/j.jngse.2015.02.009.

[19] A. Farhadian, A. S. Stoporev, M. A. Varfolomeev, Y. F. Zaripova, V. V. Yarkovoi, M. E. Semenov, A. G. Kiiamov, R. S. Pavelyev, A. M. Aimaletdinov, T. Mohammad, D. K. Nurgaliev, Sulfonated Castor Oil as an Efficient Biosurfactant for Improving Methane Storage in Clathrate Hydrates, ACS Sustain. Chem. Eng. 10 (30) (2022) 9921–9932. doi:10.1021/acssuschemeng.2c02329.

[20] X.-Y. Deng, Y. Yang, D.-L. Zhong, X.-Y. Li, B.-B. Ge, J. Yan, New Insights into the Kinetics and Morphology of CO 2 Hydrate Formation in the Presence of Sodium Dodecyl Sulfate , Energy & Fuels 35 (17) (2021) 13877–13888. doi:10.1021/acs.energyfuels.1c01494.

[21] G. Bhattacharjee, V. Barmecha, O. S. Kushwaha, R. Kumar, Kinetic promotion of methane hydrate formation by combining anionic and silicone surfactants: Scalability promise of methane storage due to prevention of foam formation, J. Chem. Thermodyn. 117 (2018) 248–255. doi:10.1016/j.jct.2017.09.029.

[22] G. Pandey, G. Bhattacharjee, H. P. Veluswamy, R. Kumar, J. S. Sangwai, P. Linga, Alleviation of Foam Formation in a Surfactant Driven Gas Hydrate System: Insights via a Detailed Morphological Study, ACS Appl. Energy Mater. 1 (12) (2018) 6899–6911. doi:10.1021/acsaem.8b01307.

[23] W. X. Pang, G. J. Chen, A. Dandekar, C. Y. Sun, C. L. Zhang, Experimental study on the scale-up effect of gas storage in the form of hydrate in a quiescent reactor, Chem. Eng. Sci. 62 (8) (2007) 2198–2208. doi:10.1016/j.ces.2007.01.001.

[24] Y. Qin, Z. Pan, Z. Liu, L. Shang, L. Zhou, Influence of the Particle Size of Porous Media on the Formation of Natural Gas Hydrate: A Review, Energy and Fuels 35 (15) (2021) 11640–11664. doi:10.1021/acs.energyfuels.1c00936.

[25] L. Borchardt, M. E. Casco, J. Silvestre-Albero, Methane Hydrate in Confined Spaces: An Alternative Storage System, ChemPhysChem 19 (11) (2018) 1298–1314. doi:10.1002/cphc.201701250.

[26] Y. Wang, X. Lang, S. Fan, Accelerated nucleation of tetrahydrofuran (THF) hydrate in presence of ZIF-61, J. Nat. Gas Chem. 21 (3) (2012) 299–301. doi:10.1016/S1003-9953(11)60367-8.

[27] M. Khurana, Z. Yin, P. Linga, A review of clathrate hydrate nucleation, ACS Sustain. Chem. Eng. 5 (12) (2017) 11176–11203. doi:10.1021/acssuschemeng.7b03238.

[28] S. Said, V. Govindaraj, J. M. Herri, Y. Ouabbas, M. Khodja, M. Belloum, J. S. Sangwai, R. Nagarajan, A study on the influence of nanofluids on gas hydrate formation kinetics and their potential: Application to the CO2 capture process, J. Nat. Gas Sci. Eng. 32 (2016) 95–108. doi:10.1016/j.jngse.2016.04.003.

[29] J. W. Choi, J. T. Chung, Y. T. Kang, CO2 hydrate formation at atmospheric pressure using high efficiency absorbent and surfactants, Energy 78 (2014) 869–876. doi:10.1016/j.energy.2014.10.081.

[30] Z. Pan, Z. Liu, Z. Zhang, L. Shang, S. Ma, Effect of silica sand size and saturation on methane hydrate formation in the presence of SDS, J. Nat. Gas Sci. Eng. 56 (February) (2018) 266–280. doi:10.1016/j.jngse.2018.06.018.

[31] S. Rungrussamee, K. Inkong, S. Kulprathipanja, P. Rangsunvigit, Comparative study of methane hydrate formation and dissociation with hollow silica and activated carbon, Chem. Eng. Trans. 70 (2018) 1519–1524. doi:10.3303/CET1870254.

[32] G. Zhang, B. Liu, L. Xu, R. Zhang, Y. He, F. Wang, How porous surfaces influence the nucleation and growth of methane hydrates, Fuel 291 (2021) 120142. doi:10.1016/j.fuel.2021.120142.

[33] Y. Peng, V. Krungleviciute, I. Eryazici, J. T. Hupp, O. K. Farha, T. Yildirim, Methane storage in metal-organic frameworks: Current records, surprise findings, and challenges, J. Am. Chem. Soc. 135 (32) (2013) 11887–11894. doi:10.1021/ja4045289.

[34] E. Mahmoud, L. Ali, A. E. Sayah, S. A. Alkhatib, H. Abdulsalam, M. Juma, A. H. Al-Muhtaseb, Implementing metal-organic frameworks for natural gas storage, Crystals 9 (8) (2019) 1–19. doi:10.3390/cryst9080406.

[35] K. Inkong, H. P. Veluswamy, P. Rangsunvigit, S. Kulprathipanja, P. Linga, Innovative Approach to Enhance the Methane Hydrate Formation at Near-Ambient Temperature and Moderate Pressure for Gas Storage Applications, Ind. Eng. Chem. Res. 58 (49) (2019) 22178–22192. doi:10.1021/acs.iecr.9b04498.

[36] X. Y. Zang, S. S. Fan, D. Q. Liang, D. L. Li, G. J. Chen, Influence of 3A molecular sieve on tetrahydrofuran (THF) hydrate formation, Sci. China, Ser. B Chem. 51 (9) (2008) 893–900. doi:10.1007/s11426-008-0035-2.

[37] X. ZANG, J. DU, D. LIANG, S. FAN, C. TANG, Influence of A-type Zeolite on Methane Hydrate Formation, Chinese J. Chem. Eng. 17 (5) (2009) 854–859. doi:10.1016/S1004-9541(08)60287-6.

[38] J.-H. H. Nam-Jin Kim, Sung-Seek Park, Sang-Woong Shin, W. Chun, An experimental investigation into the effects of zeolites on the formation of methane hydrates, Int. J. Energy Res. 39 (2015) 26–32. arXiv:arXiv:1011.1669v3, doi:10.1002/er.

[39] A. Omran, N. Nesterenko, V. Valtchev, Revealing Zeolites Active Sites Role as Kinetic Hydrate Promoters: Combined Computational and Experimental Study, ACS Sustain. Chem. Eng. 10 (24) (2022) 8002–8010. doi:10.1021/acssuschemeng.2c01742.

[40] D. Shi, G. Fu, A. Omran, K.-g. Haw, L. Zhu, R. Ding, Q. Lang, S. Wang, Q. Fang, S. Qiu, X. Yang, V. Valtchev, Acidic properties of al-rich zsm-5 crystallized in strongly acidic fluoride medium, Microporous Mesoporous Mater. 358 (November 2022) (2023) 112332. doi:10.1016/j.micromeso.2022.112332.

[41] A. Palčić, V. Valtchev, Analysis and control of acid sites in zeolites, Appl. Catal. A Gen. 606 (July 2020) (2020) 117795. doi:10.1016/j.apcata.2020.117795.

[42] S. Denning, A. A. Majid, J. M. Crawford, M. A. Carreon, C. A. Koh, Promoting Methane Hydrate Formation for Natural Gas Storage over Chabazite Zeolites, ACS Appl. Energy Mater. 4 (11) (2021) 13420–13424. doi:10.1021/acsaem.1c02902.

[43] A. Omran, N. Nesterenko, A. A. Paecklar, N. Barrier, V. Valtchev, Toward Economical Seawater-Based Methane Hydrate Formation at Ambient Temperature: A Combined Experimental and Computational Study, ACS Sustain. Chem. Eng. 10 (35) (2022) 11617–11626. doi:10.1021/acssuschemeng.2c03530.

[44] J. S. Pandey, Y. J. Daas, N. von Solms, Screening of amino acids and surfactant as hydrate promoter for CO2 capture from flue gas, Processes 8 (124) (2020) 1–23. doi:10.3390/pr8010124.

[45] S. E. Gainullin, A. Farhadian, P. Y. Kazakova, M. E. Semenov, Y. F. Chirkova, A. Heydari, R. S. Pavelyev, M. A. Varfolomeev, Novel amino acid derivatives for efficient methane solidification storage via clathrate hydrates without foam formation, Energy & Fuels 37 (4) (2023) 3208–3217.

[46] N. N. Nguyen, M. Galib, A. V. Nguyen, Critical Review on Gas Hydrate Formation at Solid Surfaces and in Confined Spaces—Why and How Does Interfacial Regime Matter?, Energy & Fuels 34 (6) (2020) 6751–6760. doi:10.1021/acs.energyfuels.0c01291.

[47] A. A. Majid, J. Worley, C. A. Koh, Thermodynamic and Kinetic Promoters for Gas Hydrate Technological Applications, Energy and Fuels 35 (23) (2021) 19288–19301. doi:10.1021/acs.energyfuels.1c02786.

[48] H. Roosta, A. Dashti, S. Hossein Mazloumi, F. Varaminian, The dual effect of amino acids on the nucleation and growth rate of gas hydrate in ethane + water, methane + propane + water and methane + THF + water systems, Fuel 212 (2017) 151–161. doi:10.1016/j.fuel.2017.10.027.

[49] Q. Nasir, H. Suleman, Y. A. Elsheikh, A review on the role and impact of various additives as promoters/ inhibitors for gas hydrate formation, J. Nat. Gas Sci. Eng. 76 (February) (2020) 103211. doi:10.1016/j.jngse.2020.103211.

[50] J. H. Sa, G. H. Kwak, B. R. Lee, D. H. Park, K. Han, K. H. Lee, Hydrophobic amino acids as a new class of kinetic inhibitors for gas hydrate formation, Sci. Rep. 3 (2013) 1–7. doi:10.1038/srep02428.

[51] C. B. Bavoh, B. Lal, H. Osei, K. M. Sabil, H. Mukhtar, A review on the role of amino acids in gas hydrate inhibition, CO2 capture and sequestration, and natural gas storage, J. Nat. Gas Sci. Eng. 64 (November 2018) (2019) 52–71. doi:10.1016/j.jngse.2019.01.020.

[52] P. Linga, N. Daraboina, J. A. Ripmeester, P. Englezos, Enhanced rate of gas hydrate formation in a fixed bed column filled with sand compared to a stirred vessel, Chem. Eng. Sci. 68 (1) (2012) 617–623. doi:10.1016/j.ces.2011.10.030.

[53] P. Linga, M. A. Clarke, A Review of Reactor Designs and Materials Employed for Increasing the Rate of Gas Hydrate Formation, Energy Fuels 31 (2017) 30. doi:10.1021/acs.energyfuels.6b02304.

[54] Z. Yin, M. Khurana, H. K. Tan, P. Linga, A review of gas hydrate growth kinetic models (2018). doi:10.1016/j.cej.2018.01.120.

[55] J. Zheng, B.-Y. Zhang, Q. Wu, P. Linga, Kinetic Evaluation of Cyclopentane as a Promoter for CO 2 Capture via a Clathrate Process Employing Different Contact Modes, ACS Sustain. Chem. Eng. 6 (9) (2018) 11913–11921. doi:10.1021/acssuschemeng.8b02187.

[56] M. R. Ghaani, J. M. Schicks, N. J. English, A review of reactor designs for hydrogen storage in clathrate hydrates, Appl. Sci. 11 (2) (2021) 1–16. doi:10.3390/app11020469.

[57] P. Babu, P. Linga, R. Kumar, P. Englezos, A review of the hydrate based gas separation (HBGS) process for carbon dioxide pre-combustion capture, Energy 85 (2015) 261–279. doi:10.1016/j.energy.2015.03.103.

[58] A. Kumar, R. Kumar, Role of metallic packing and kinetic promoter in designing a hydrate-based gas separation process, Energy and Fuels 29 (7) (2015) 4463–4471. doi:10.1021/acs.energyfuels.5b00664.

[59] A. Heydari, K. Peyvandi, Role of metallic porous media and surfactant on kinetics of methane hydrate formation and capacity of gas storage, J. Pet. Sci. Eng. 181 (July) (2019) 106235. doi:10.1016/j.petrol.2019.106235.

[60] N. Gaikwad, G. Bhattacharjee, O. S. Kushwaha, J. S. Sangwai, P. Linga, R. Kumar, Effect of Cyclooctane and L-Tryptophan on Hydrate Formation from an Equimolar CO2–CH4 Gas Mixture Employing a Horizontal-Tray Packed Bed Reactor, Energy & Fuels 34 (8) (2020) 9840–9851. doi:10.1021/acs.energyfuels.0c01511.

[61] N. B. Kummamuru, S. W. Verbruggen, S. Lenaerts, P. Perreault, Experimental investigation of methane hydrate formation in the presence of metallic packing, Fuel 323 (February) (2022) 124269. doi:10.1016/j.fuel.2022.124269.

[62] B. K. Steven H. Kosmatka, W. C. Panarese, Design and Control of Concrete Mixtures The Guide to Applications, Methods and Materials., 14th Edition, 2008.

[63] F. E. Jones, R. M. Schoonover, Handbook of mass measurement, Chapman and Hall/CRC, 2002. doi:10.1201/9781420038453.

[64] L. Yang, C. Li, J. Pei, X. Wang, N. Liu, Y. Xie, G. Cui, D. Liu, Enhanced clathrate hydrate phase change with open-cell copper foam for efficient methane storage, Chem. Eng. J. 440 (December 2021) (2022) 135912. doi:10.1016/j.cej.2022.135912.

[65] Z. Pan, Z. Liu, Z. Zhang, L. Shang, S. Ma, Effect of silica sand size and saturation on methane hydrate formation in the presence of SDS, J. Nat. Gas Sci. Eng. 56 (February) (2018) 266–280. doi:10.1016/j.jngse.2018.06.018.

[66] G. Bhattacharjee, H. Prakash, A. Kumar, P. Linga, Stability analysis of methane hydrates for gas storage application, Chem. Eng. J. 415 (December 2020) (2021) 128927. doi:10.1016/j.cej.2021.128927.

[67] S. Takeya, T. Uchida, J. Nagao, R. Ohmura, W. Shimada, Y. Kamata, T. Ebinuma, H. Narita, Particle size effect of CH4 hydrate for self-preservation 60 (2005) 1383–1387. doi:10.1016/j.ces.2004.10.011.

[68] S. Takeya, A. Yoneyama, K. Ueda, K. Hyodo, T. Takeda, H. Mimachi, M. Takahashi, T. Iwasaki, K. Sano, H. Yamawaki, Y. Gotoh, Nondestructive Imaging of Anomalously Preserved Methane Clathrate Hydrate by Phase Contrast X-ray Imaging (2011) 16193–16199.

[69] H. Mimachi, M. Takahashi, S. Takeya, Y. Gotoh, A. Yoneyama, K. Hyodo, T. Takeda, T. Murayama, Effect of Long-Term Storage and Thermal History on the Gas Content of Natural Gas Hydrate Pellets under Ambient Pressure (2015). doi:10.1021/acs.energyfuels.5b00832.

[70] Martin, Philippe, B. W. di Mauro, Winter is coming: Energy policy towards Russia, CEPR PRESS Centre, 2022. doi:10.5167/uzh-222702.

[71] W. Kohn, Nobel lecture: Electronic structure of matter - Wave functions and density functional, Rev. Mod. Phys. 71 (5) (1999) 1253–1266. doi:10.1103/revmodphys.71.1253.

[72] A. S. Omran, DFT Study of Copper-Nickel (111) Catalyst for Methane Dry Reforming, Ph.D. thesis, (Master Disseration)Texas A & M (2019). arXiv:arXiv:1011.1669v3.

[73] P. Giannozzi, S. Baroni, N. Bonini, M. Calandra, R. Car, C. Cavazzoni, D. Ceresoli, G. L. Chiarotti, M. Cococcioni, I. Dabo, A. Dal Corso, S. De Gironcoli, S. Fabris, G. Fratesi, R. Gebauer, U. Gerstmann, C. Gougoussis, A. Kokalj, M. Lazzeri, L. Martin-Samos, N. Marzari, F. Mauri, R. Mazzarello, S. Paolini, A. Pasquarello, L. Paulatto, C. Sbraccia, S. Scandolo, G. Sclauzero, A. P. Seitsonen, A. Smogunov, P. Umari, R. M. Wentzcovitch, QUANTUM ESPRESSO: A modular and open-source software project for quantum simulations of materials, J. Phys. Condens. Matter 21 (39) (2009) 395502. arXiv:0906.2569, doi:10.1088/0953-8984/21/39/395502.

[74] T. M. Vlasic, P. D. Servio, A. D. Rey, THF Hydrates as Model Systems for Natural Gas Hydrates: Comparing Their Mechanical and Vibrational Properties, Ind. Eng. Chem. Res. 58 (36) (2019) 16588–16596. doi:10.1021/acs.iecr.9b02698.

[75] A. Omran, N. Nesterenko, V. Valtchev, Revealing Acidic Zeolites: Role as New Kinetic Hydrate Promoters: A Combined Computational and Experimental Study, in: 37th meeting of French Group of Zeolite (GFZ), Vogüé, France, 2022.

[76] A. Kumar, H. P. Veluswamy, P. Linga, R. Kumar, Molecular level investigations and stability analysis of mixed methane-tetrahydrofuran hydrates: Implications to energy storage, Fuel 236 (August 2018) (2019) 1505–1511. doi:10.1016/j.fuel.2018.09.126.

[77] D. Lee, W. Go, Y. Seo, Experimental and computational investigation of methane hydrate inhibition in the presence of amino acids and ionic liquids, Energy 182 (2019) 632–640. doi:10.1016/j.energy.2019.06.025.

[78] M. Tariq, D. Rooney, E. Othman, S. Aparicio, M. Atilhan, M. Khraisheh, Gas hydrate inhibition: A review of the role of ionic liquids, Ind. Eng. Chem. Res. 53 (46) (2014) 17855–17868. doi:10.1021/ie503559k.

[79] M. Atilhan, N. Pala, S. Aparicio, A quantum chemistry study of natural gas hydrates, J. Mol. Model. 20 (4) (2014) 1–15. doi:10.1007/s00894-014-2182-z.

[80] C. B. Bavoh, B. Lal, H. Osei, K. M. Sabil, H. Mukhtar, A review on the role of amino acids in gas hydrate inhibition, CO2 capture and sequestration, and natural gas storage, J. Nat. Gas Sci. Eng. 64 (November 2018) (2019) 52–71. doi:10.1016/j.jngse.2019.01.020.

[81] D. Lee, W. Go, G. Ko, Y. Seo, Inhibition synergism of glycine (an amino acid) and [BMIM][BF4] (an ionic liquid) on the growth of CH4 hydrate, Chem. Eng. J. 393 (February) (2020) 124466. doi:10.1016/j.cej.2020.124466.

[82] P. S. Prasad, B. S. Kiran, Are the amino acids thermodynamic inhibitors or kinetic promoters for carbon dioxide hydrates?, J. Nat. Gas Sci. Eng. 52 (January) (2018) 461–466. doi:10.1016/j.jngse.2018.02.001.

[83] Y. Cai, Y. Chen, Q. Li, L. Li, H. Huang, S. Wang, W. Wang, CO2 Hydrate Formation Promoted by a Natural Amino Acid l-Methionine for Possible Application to CO2 Capture and Storage, Energy Technol. 5 (8) (2017) 1195–1199. doi:10.1002/ente.201600731.

[84] H. P. Veluswamy, A. Kumar, R. Kumar, P. Linga, An innovative approach to enhance methane hydrate formation kinetics with leucine for energy storage application, Appl. Energy 188 (2017) 190–199. doi:10.1016/j.apenergy.2016.12.002.

[85] N. N. Nguyen, A. V. Nguyen, Hydrophobic Effect on Gas Hydrate Formation in the Presence of Additives, Energy and Fuels 31 (10) (2017) 10311–10323. doi:10.1021/acs.energyfuels.7b01467.

[86] J. Kyte, R. F. Doolittle, A simple method for displaying the hydropathic character of a protein, J. Mol. Biol. 157 (1) (1982) 105–132. doi:10.1016/0022-2836(82)90515-0.

[87] A. Desmedt, L. Martin-Gondre, T. T. Nguyen, C. Pétuya, L. Barandiaran, O. Babot, T. Toupance, R. G. Grim, A. K. Sum, Modifying the flexibility of water cages by co-including acidic species within clathrate hydrate, J. Phys. Chem. C 119 (16) (2015) 8904–8911. doi:10.1021/jp511826b.

[88] T. T. Nguyen, C. Pétuya, D. Talaga, A. Desmedt, Promoting the Insertion of Molecular Hydrogen in Tetrahydrofuran Hydrate With the Help of Acidic Additives, Front. Chem. 8 (2020) 550862. doi:10.3389/fchem.2020.550862.

[89] G. N. Vayssilov, H. A. Aleksandrov, E. Dib, I. M. Costa, N. Nesterenko, S. Mintova, Superacidity and spectral signatures of hydroxyl groups in zeolites, Microporous Mesoporous Mater. 343 (August) (2022) 112144. doi:10.1016/j.micromeso.2022.112144.

[90] K. Inkong, P. Rangsunvigit, S. Kulprathipanja, P. Linga, Effects of temperature and pressure on the methane hydrate formation with the presence of tetrahydrofuran (THF) as a promoter in an unstirred tank reactor, Fuel 255 (May) (2019) 115705. doi:10.1016/j.fuel.2019.115705.

[91] N. B. Kummamuru, S. W. Verbruggen, S. Lenaerts, P. Perreault, Experimental investigation of methane hydrate formation in the presence of metallic packing, Fuel 323 (April) (2022) 124269. doi:10.1016/j.fuel.2022.124269.

[92] H. P. Veluswamy, A. J. H. Wong, P. Babu, R. Kumar, S. Kulprathipanja, P. Rangsunvigit, P. Linga, Rapid methane hydrate formation to develop a cost effective large scale energy storage system, Chem. Eng. J. 290 (2016) 161–173. doi:10.1016/j.cej.2016.01.026.

[93] N. N. Nguyen, Prospect and challenges of hydrate-based hydrogen storage in the low-carbon future, Energy & Fuels.

[94] B. Lucia, B. Castellani, F. Rossi, F. Cotana, E. Morini, A. Nicolini, M. Filipponi, Experimental investigations on scaled-up methane hydrate production with surfactant promotion: Energy considerations, J. Pet. Sci. Eng. 120 (2014) 187–193. doi:10.1016/j.petrol.2014.06.015.

[95] Y. Zhang, G. Bhattacharjee, M. Dharshini Vijayakumar, P. Linga, Rapid and energy-dense methane hydrate formation at near ambient temperature using 1,3-dioxolane as a dual-function promoter, Appl. Energy 311 (February) (2022) 118678. doi:10.1016/j.apenergy.2022.118678.

[96] A. Kumar, R. Kumar, P. Linga, Sodium Dodecyl Sulfate Preferentially Promotes Enclathration of Methane in Mixed Methane-Tetrahydrofuran Hydrates (2019). doi:10.1016/j.isci.2019.03.020.

[97] I. Lee, J. Park, I. Moon, Key Issues and Challenges on the Liquefied Natural Gas Value Chain: A Review from the Process Systems Engineering Point of View, Ind. Eng. Chem. Res. 57 (17) (2018) 5805–5818. doi:10.1021/acs.iecr.7b03899.

[98] M. M. F. Hasan, A. M. Zheng, I. A. Karimi, Minimizing Boil-Off Losses in Liquefied Natural Gas Transportation, Ind. Eng. Chem. Res. 48 (21) (2009) 9571–9580. doi:10.1021/ie801975q.

[99] A. Kumar, T. Sakpal, P. Linga, R. Kumar, Enhanced carbon dioxide hydrate formation kinetics in a fixed bed reactor filled with metallic packing, Chem. Eng. Sci. 122 (2015) 78–85. doi:10.1016/j.ces.2014.09.019.

[100] H. Pahlavanzadeh, S. Rezaei, M. Khanlarkhani, M. Manteghian, A. H. Mohammadi, Kinetic study of methane hydrate formation in the presence of copper nanoparticles and CTAB, J. Nat. Gas Sci. Eng. 34 (2016) 803–810. doi:10.1016/j.jngse.2016.07.001.

[101] P. Linga, M. A. Clarke, A Review of Reactor Designs and Materials Employed for Increasing the Rate of Gas Hydrate Formation, Energy & Fuels 31 (1) (2017) 1–13. doi:10.1021/acs.energyfuels.6b02304.

[102] M. Aifaa, T. Kodama, R. Ohmura, Crystal growth of clathrate hydrate in a flowing liquid water system with methane gas, Cryst. Growth Des. 15 (2) (2015) 559–563. doi:10.1021/cg500992c.

[103] D. Gootam, N. Gaikwad, R. Kumar, N. Kaisare, Modeling Growth Kinetics of Methane Hydrate in Stirred Tank Batch Reactors, ACS Eng. Au 1 (2) (2021) 148–159. doi:10.1021/acsengineeringau.1c00012.

[104] Y. H. Mori, On the scale-up of gas-hydrate-forming reactors: The case of gas-dispersion-type reactors, Energies 8 (2) (2015) 1317–1335. doi:10.3390/en8021317.

[105] W. Hao, J. Wang, S. Fan, W. Hao, Evaluation and analysis method for natural gas hydrate storage and transportation processes, Energy Convers. Manag. 49 (10) (2008) 2546–2553. doi:10.1016/j.enconman.2008.05.016.

[106] F. Rossi, M. Filipponi, B. Castellani, Investigation on a novel reactor for gas hydrate production, Appl. Energy 99 (Icgh) (2012) 167–172. doi:10.1016/j.apenergy.2012.05.005.